Illek, D. Livshits, A. Rucki, M. Schuster, A. Kaschner, A. Hoffmann, Gh. Dumitras, M.C. Amann, and H. Riechert, "Growth of high quality InGaAsN heterostructures and their laser application," J. Crystal Growth 227–228, 545–552 (2001).

5. W. Li, M. Pessa, T. Ahlgren, and J. Decker, "Origin of improved luminescence efficiency after annealing of GaInNAs materials grown by molecular beam epitaxy," Appl. Phys. Lett. 79, 1094–1096 (2001).

CTuQ4 **3:30 pm**

Temperature Sensitivity Analysis of High-performance InGaAs(N) (λ = 1.185 – 1.3 μm) Quantum Well Lasers

Nelson Tansu, and Luke J. Mawst, Department of Electrical Computer Engineering, University of Wisconsin-Madison, 1415 Engineering Dr., Madison, WI, 53706, USA, Email: tansu@cae.wisc.edu

InGaAsN QW active lasers, proposed by Kondow et. al.,[1] have shown strong potential for temperature-insensitive optical transmitters at $\lambda = 1.3$ μm used in metropolitan optical network systems. Here we demonstrate low-threshold-current MOCVD-grown diode lasers, as shown in Fig. 1, utilizing 60-Å $In_{0.4}Ga_{0.6}As$ QW and 60-Å $In_{0.4}Ga_{0.6}As_{0.995}N_{0.005}$ QW active layers, with strain compensating $GaAs_{0.85}P_{0.15}$ (tensile) barriers and a (tensile) InGaP ($\Delta a/a$ = –700 ppm) buffer layer.[2] We find the use of a tensile-strained InGaP buffer layer to be crucial for the growth of the high-In-content InGaAs(N) QWs on a thick high-Al-content AlGaAs bottom-cladding layers, as evident from the significant improvement in the luminescence from incorporation of the buffer layer.[2] The InGaAs QW laser, with λ = 1.185 μm, exhibits threshold and transparency current densities as low as 100A/cm^2 (L = 2000-μm) and 59A/cm^2, respectively, with an internal quantum efficiency of 80%. Low threshold and transparency current density, as low as 289 A/cm^2(L = 1500-μm) and 110 A/cm^2, respectively is also obtained for the InGaAsN QW lasers (λ = 1.295 μm), with an internal quantum efficiency 72%. Both InGaAs-QW and InGaAsN-QW lasers exhibit high external differential quantum efficiency of 63% (L = 500-μm) and 51% (L = 750-μm), respectively.

A temperature analysis (20°C–60°C) is performed to understand further the temperature dependent mechanisms for both InGaAs and InGaAsN QW lasers. The characteristic temperature coefficients of the threshold current density (T_o) and external differential quantum efficiency (T_1) are studied as functions of the physical device parameters and their temperature dependence, which can be expressed as follows[3]

$$\frac{1}{T_o(L)} = \frac{1}{T_{tr}} + \frac{1}{T_{\eta i}} + \frac{\alpha_i + \alpha_m(L)}{\Gamma \cdot g_o} \cdot \left(\frac{1}{T_{go}} + \frac{\alpha_i}{\alpha_i + \alpha_m(L)} \cdot \frac{1}{T_{\alpha i}} \right) \quad (1),$$

$$\frac{1}{T_1(L)} = \frac{1}{T_{\eta i}} + \frac{\alpha_i}{\alpha_i + \alpha_m(L)} \cdot \frac{1}{T_{\alpha i}} \quad (2)$$

with T_{tr}, $T_{\eta i}$, T_{go}, and $T_{\alpha i}$ being the characteristic temperature coefficients of the transparency current density, internal quantum efficiency, material gain parameter, and internal loss, respectively.

The T_o values of the InGaAs QW lasers are measured to be in excess of 200 K, for 500–2000 μm cavity length devices. By contrast, we observed significantly lower T_o values for the InGaAsN lasers, with T_o values of 110–130 K for 500–1500 μm cavity-length devices. Based on the measured temperature dependence of the transparency current density (T_{tr}),[3] as shown in Fig. 2(a), we are able to identify that Auger recombination is minimal for both InGaAs QW (T_{tr} = 280 K) and InGaAsN QW (T_{tr} = 285 K) lasers. Low Auger recombination, in InGaAsN QW lasers, has also been reported by Fehse, et. al.,[4] using pressure dependent measurements. In contrast to that ($T_{\alpha i}$ ~ 90–100 K) of InP-based 1.3-μm lasers,[5] the values of $T_{\alpha i}$ are measured to be as high as 500–1200 K, which indicates minimal IVBA loss in both InGaAs QW and InGaAsN QW lasers. The internal loss of the InGaAs and InGaAsN lasers are measured to be 6-cm^{-1} and 6.9-cm^{-1}, respectively. By comparison to InP-based 1.3-μm lasers, the material gain parameters for both InGaAs and InGaAsN lasers are very temperature insensitive, with T_{go} values in excess of 350 K. We attribute the primary mechanism of the lower T_o value for InGaAsN QW lasers to be the stronger temperature dependence of the carrier injection efficiency ($T_{\eta i}$ = 500 K), as shown in Fig. 2(b). Presumably this could be a result of larger hole carrier-leakage, from the InGaAsN QW, due to the large disparity in the conduction- and valence-band offset and higher threshold carrier-density, compared to that of the InGaAs QW ($T_{\eta i}$ = 950 K).

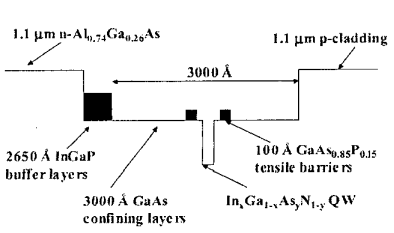

CTuQ4 Fig. 1. Schematic energy bandgap diagram for the InGaAs(N)-GaAsP-GaAs QW laser structures.

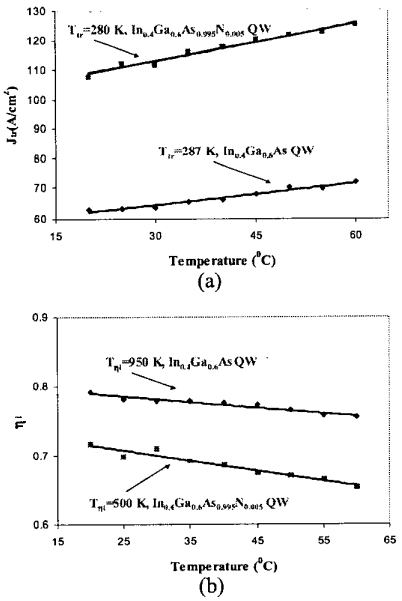

CTuQ4 Fig. 2. The transparency current density (a) and the carrier injection efficiency (b) of strain-compensated $In_{0.4}Ga_{0.6}As$ QW and $In_{0.4}Ga_{0.6}As_{0.995}N_{0.005}$ QW lasers, as functions of temperature.

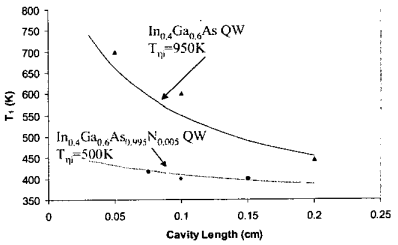

CTuQ4 Fig. 3. The measured characteristic temperature coefficient of the external differential quantum efficiency (T_1) for strain-compensated $In_{0.4}Ga_{0.6}As$ QW and $In_{0.4}Ga_{0.6}As_{0.995}N_{0.005}$ QW lasers, as functions of cavity-length, with the lines represent the predicted T_1 values from eq. (2).

The temperature dependence of the external differential quantum efficiency (T_1), as shown in Fig. 3, depends on the values of $T_{\eta i}$ $T_{\alpha i}$, and the total losses. The T_1 values vary with cavity length, due to differences in the required threshold modal gain.

References

1. M. Kondow, T. Kitatani, S. Nakatsuka, M.C. Larson, K. Nakahara, Y. Yazawa, M. Okai, and K. Uomi, *IEEE J. Select. Topic Quantum Electronic.*, vol. 3, pp. 719–730, 1997.
2. N. Tansu and L.J. Mawst, *IEEE Photon. Technol. Lett.*, (submitted).
3. N. Tansu, Y.L. Chang, T. Takeuchi, D.P. Bour, S.W. Corzine, M.R.T. Tan, and L.J. Mawst, *IEEE. J. Quantum Electron.* (submitted).
4. R. Fehse, S.J. Sweeney, A.R. Adams, E.P. O'Reilly, A.Y. Egorov, H. Riechert, and S. Illek, *Electron. Lett.*, 37(2), pp. 92–93, 2000.
5. A.F. Phillips, A.F. Sweeney, A.R. Adams, and P.J.A. Thijs, *IEEE. J. Select. Topics Quantum Electron.*, Vol. 5, No. 3, pp. 401–412, May/June 1999.

CTuQ5 **3:45 pm**

Long Wavelength GaInNAs(Sb) Lasers on GaAs

Wonill Ha, Vincent Gambin, Seth Bank, Mark Wistey, James S. Harris Jr., Solid State and Photonics Lab., CISX B113-3, Via Ortega, Stanford University, Stanford, CA 94305 USA

Seongsin Kim, Agilent Technologies Inc., San Jose, CA 95131 USA

There is now a very high demand for low cost, 1.3–1.6 μm lasers that are essential for the rapid expansion of optical metro area networks (MANs). The requirements for these lasers are a significant operating temperature range (–10 to 90°C), emission spectra over 1.3–1.6 μm, and

moderate power (>10 mW). There is also a significant interest in higher power lasers as Raman pumps to greatly increase the available bandwidth. InP-based lasers have serious shortcomings that hinder their ability to cover the 1.3–1.6 μm wavelength range,[1] both for low cost vertical-cavity surface-emitting lasers (VCSELs) and high-power Raman pumps. Recent work on GaAs-based lasers with nitrogen has demonstrated promising results in light of the considerable improvement in thermal properties, the advantages of GaAs-based processing techniques, and the superior DBR (Distributed Bragg Reflector) mirror technology available for VCSELs. Much research has now been done showing that GaInNAs, that is nearly lattice matched to GaAs,[2–4] can have a bandgap energy in the long wavelength range. GaInNAs has shown prospective characteristics, including low threshold current density, high temperature CW operation, and high T_0 in the wavelength range of 1.1 μm to 1.3 μm.

We present a new structure utilizing antimony, either incorporated into the crystal or used as a surfactant, to enable higher nitrogen and indium incorporation. This results in a shift of the post-annealed emission to longer wavelengths. The material for this study was grown by MBE with an RF plasma source. In contrast to conventional GaAs barriers between GaInNAs quantum wells, we utilize GaNAs and GaNAs(Sb) barriers with GaInNAs(Sb) quantum wells (QWs). This design reduces the blue-shift of the emission spectrum by reducing nitrogen out-diffusion in the QWs. GaNAs(Sb) barriers can also reduce the overall strain of the active region (GaInNAs(Sb) quantum wells and GaNAs(Sb) barriers) because the high In mole fraction QWs are compressively strained and the GaNAs barriers are tensily strained. With GaNAs barriers, we were able to grow samples with nine quantum wells (63 nm QW thickness), which is well above the critical thickness. A nine QW photoluminescence (PL) sample shows approximately 3 times stronger PL intensity than a three QW sample and is applicable to high power lasers. With GaNAs(Sb) barriers, we were able to incorporate up to 46% indium with total active layer thickness of 21 nm. We will present results of high efficiency long wavelength multiple quantum well (MQW) GaInNAs ridge-waveguide laser diodes using GaNAs barriers (Fig. 1). We will also show GaInNAs(Sb)/GaNAs(Sb) ridge waveguide laser with emission at 1.465 μm, as seen in Fig. 3. We have observed photoluminescence (Fig. 2) up to 1.6 μm with different indium and antimony concentrations. Our GaInNAs and GaInNAs(Sb) ridge waveguide laser diodes have broad emission spectra covering 1.27 μm to 1.465 μm with pulsed operation up to 90°C. The maximum output power at room temperature, under pulsed operation (1 μs duration, 1% duty cycle), was 320 mW with a differential efficiency of 0.67W/A. We believe that these ridge waveguide lasers are ideally suited for broad bandwidth communication sources, as well as for Raman pumps.

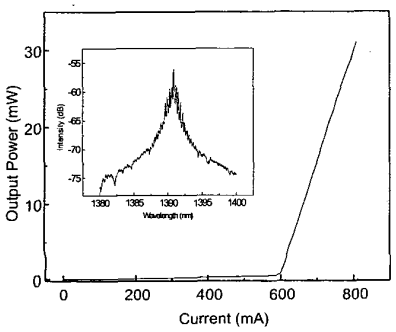

CTuQ5 Fig. 1. L-I curve and optical spectrum for a GaInNAs/GaNAs ridge waveguide laser with peak emission at 1.39 μm.

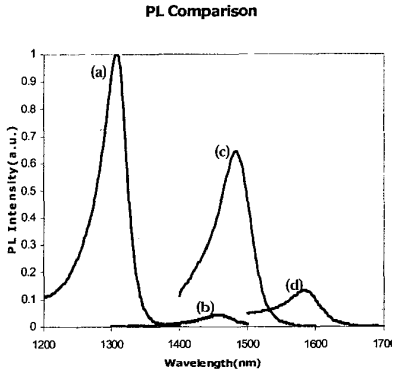

CTuQ5 Fig. 2. Photoluminescence of various GaInNAs(Sb) samples normalized to (a) the highest 1.3 μm peak. (b) 44% In and an Sb flux of 4.6×10^{-8} torr, (c) 45% In and an Sb flux of 7.2×10^{-8} torr, (d) 46% In and an Sb flux of 1.7×10^{-7} torr.

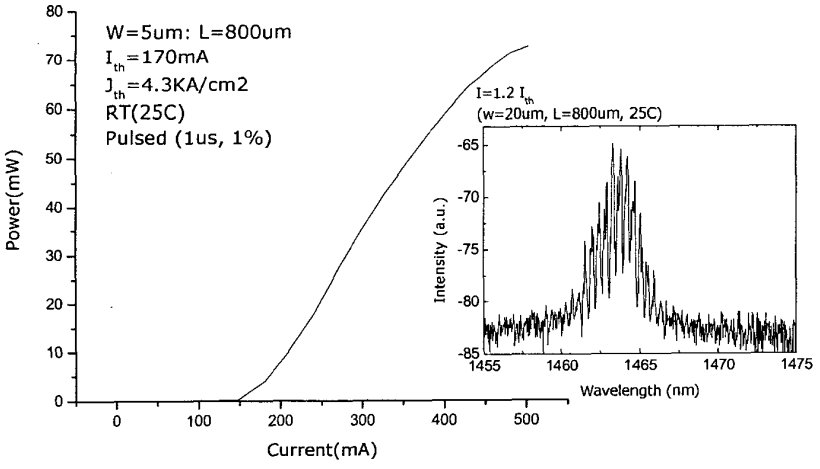

CTuQ5 Fig. 3. L-I curve and optical spectrum for a GaInNAs(Sb)/GaNAs(Sb) ridge waveguide laser with peak emission at 1.463 μm. The In mole fraction is 0.44 and Sb flux was 6.86×10^{-8} torr.

References

1. Phillips, A.F., Sweeney, S.J., Adams, A.R., and Thijs, P.J.A., "The temperature dependence of 1.3 and 1.55 μm compressively strained InGaAs(P) MQW semiconductor lasers," *IEEE J. Select. Topics Quantum Electron.*, 5, 301, (1999).
2. M. Kondow, T. Kitatani, S. Nakatsuka, M.C. Larson, K. Nakahara, Y. Yazawa, M. Okai and K. Uomi, "GaInNAs: A novel material for long wavelength semiconductor lasers," *IEEE J. Select. Topics Quantum Electron.*, 3, 719, (1997).
3. S. Sato, Y. Osawa, T. Saitoh, and I. Fujimura, "Room-temperature pulsed operation of 1.3 μm GaInNAs/GaAs laser diode," *Electro. Lett.*, 33, 1386, July (1997).
4. Gokhale, M.R., Studentkov, P.V., Wei J., and Forrest, S.R., "Low threshold current, high efficiency 1.3 μm wavelength aluminium-free InGaAsN-based quantum-well lasers," *IEEE Photonics Tech. Lett.* 12, 131, (2000).

CTuR

4:45 pm–6:30 pm
Room: 101A

Photorefractive and Photo-EMF Effects

Marvin B. Klein, Lasson Technologies, USA, Presider

CTuR1 **4:45 pm**

Compensated Photorefractive Phase Demodulator for Probing Object in Rapid Motion

A. Blouin, C. Padioleau, D. Drolet, J.-P. Monchalin, Industrial Materials Institute, National Research Council Canada, 75, de Mortagne, Boucherville, Canada, J4B 6Y4, Email: alain.blouin@nrc.ca

Two-beam adaptive phase demodulators are used for noncontact and non-invasive measurements of the small surface displacements produced by ultrasonic waves propagating in an object. As an example the setup of a two-wave mixing-based photorefractive demodulator is shown in figure 1. These devices are based on the illumination of the surface of the object by a probing laser, collection of the light scattered by the surface of the object and its mixing with a beam directly derived from the laser (the pump beam). They are adaptive in the sense they can operate with light scattered by rough surfaces and having speckles and in the presence of various ambient perturbations. The